Electronic Supplementary Material (ESI) for Environmental Science: Processes & Impacts.
This journal is © The Royal Society of Chemistry 2015

Supplementary Material for

Effects of pH and dissolved oxygen on the photodegradation of 17α-ethynylestradiol in dissolved humic acid solution

Dong Ren, Bin Huang, Tingting Bi, Dan Xiong, Xuejun Pan*

Faculty of Environmental Science and Engineering, Kunming University of Science and Technology, Kunming, Yunnan 650500, China

* Corresponding author
E-mail address: xjpan@kmust.edu.cn

NUMBER OF PAGES: 25
NUMBER OF TEXTS: 3
NUMBER OF TABLES: 4
NUMBER OF FIGURES: 7

Text S1: Extraction procedures of local humic acid (HA)

Two liters sediments were collected by a stainless-steel Van Veen grab from each national surface water quality control point in Dianchi Lake (centered around 24°48′2″N, 102°40′17″E), China in March 2015. The collected 20 L sediments were mixed together, transported in an ice box and freeze dried upon arrival at laboratory. Finally, the freeze dried sediments were ground, passed through a 2.0 mm sieve and stored in dark conditions for extracting HA.

HA was obtained by the following extraction procedures. Briefly, a base solution (0.1 M NaOH and 0.1 M $Na_4P_2O_7$) was added into the ground sediment at a solid-liquid ratio of 20:1. The mixture was placed in dark for 24 h and stirred every 8 h. After that, the mixture was centrifuged at 2327 *g* for 15 min, and the supernatant was decanted. This extraction procedure was repeated several times until a light yellow extract was reached.

The extracted supernatants were mixed together and lowered pH to 2.0 with concentrated HCl for precipitation HA for 24 h. The mixture was then centrifuged at 2327 g for 15 min to separate HA from the solutions. The separated HA was re-dissolved in alkaline solution and precipitated with HCl, and this procedure was repeated three times. The obtained HA was demineralized three times by stirring in 0.1 M HCl and 0.3 M HF solution for 24 h under a nitrogen atmosphere. Finally, the HA was washed with Milli-Q water until a negative test of chloride using $AgNO_3$, freeze dried and crushed into particle size lower than 500 μm.

Text S2: Detection of the steady state concentration of HO· and $^1O_2$

Determination of steady state concentration of HO·

In order to quantify the steady-state concentration of HO· photogenerated by HA, terephthalic acid (TPA) was used to trap HO· producing 2-hydroxyl terephthalic acid (2-hTPA). TPA (0.3 mM) and HA (5 mg L^{-1}) solutions were prepared and irradiated under the condition as EE2 photodegradation. The hydroxylation reaction yield of 2-hTPA was reported to be 35% [1]. The concentration of 2-hTPA was detected by HPLC-Fluorescence (ex/em = 315/425 nm). Thus, the observed formation rate of 2-hTPA could be converted to HO· concentration by dividing TPA concentration, reaction yield and hydroxylation reaction rate constant according to the following Eqs. (1) ~ (3).

$$TPA + HO\cdot \rightarrow 2 - hTPA \qquad (1)$$

$$\frac{d\,[2\text{ - }hTPA]}{dt} = k_{TPA,HO\cdot}[TPA][HO\cdot]_{ss} \qquad (2)$$

$$[HO\cdot]_{ss} = \frac{d\,[2\text{ - }hTPA]}{0.35k_{TPA,HO\cdot}[TPA]dt} \qquad (3)$$

where the $k_{TPA,HO\cdot}$ is the rate constant of the reaction between TPA and HO· [2], 4.4×10^9 M^{-1} s^{-1}. The $[HO\cdot]_{ss}$ was calculated to be 4.83×10^{-15} M according to the fitted slop in Figure S2.

Determination of steady state concentration of $^1O_2$

Steady-state concentration of $^1O_2$ in HA/air (5 mg L^{-1}) system was measured by FFA probe. The reaction rate between FFA and $^1O_2$ can be depicted by Eq. (4)

$$r = k_{FFA,{}^1O_2}[1O2]_{ss}[FFA] \qquad (4)$$

where the $k_{FFA,{}^1O_2}$ is the rate constant of the reaction between FFA and $^1O_2$, 1.2 × 10^8 M^{-1} s^{-1} [3]; *r* is the observed degradation rate of FFA; [FFA] and $[^1O_2]ss$ are the concentration of FFA and $^1O_2$, respectively.

In this study, [FFA] was high enough to ignore its fluctuation. Thus, the concentration of $^1O_2$ is the rate-determining factor for FFA degradation, and the Eq. (4) can be simplified as Eq. (5).

$$r = k_{FFA,{}^1O_2}[1O2]_{ss} \qquad (5)$$

The loss of furfuryl alcohol (FFA) in the irradiated 5.0 mg L^{-1} HA solutions exposed to air follows pseudo-first order kinetics with an observed rate constant 0.1425 h^{-1} (Figure S3). $^1O_2$ in humic substance solutions can usually reach a steady-state concentration in a short term. Therefore, the concentration of $^1O_2$ could be obtained by Eq. (6), and it was calculated to be 2.04 × 10^{-13} M.

$$[1O2]_{ss} = \frac{r_{indirect} - r_{direct}}{k_{FFA,{}^1O_2}} \qquad (6)$$

Text S3: Determination of the reaction rate constants of HO· and $^1O_2$ towards EE2

Detection of the reaction rate between EE2 and HO·

The second-order reaction rate constant between EE2 and HO· was measured by a competition reaction kinetics method [4] taking benzoic acid (BZA) as a competitor for HO·. In order to avoid the influence of photodegradation on the loss of BZA, competition reactions were conducted under dark condition by taking 20 μM Fe^{2+} and 50 μM H_2O_2 (pH 3.5, adjusted by 1 M H_2SO_4) as HO· generating source. Initial concentration of BZA and EE2 was 4.68 μM and 3.84 μM, respectively. The changes in the concentration of BZA and EE2 were listed in Table S1. The kinetics expression for the depletion of the target chemicals can be given by Eqs. (7) and (8).

$$\frac{d\,[BZA]}{dt} = k_{BZA,{}^1O_2}[BZA][HO\cdot]_{SS} \qquad (7)$$

$$\frac{d\,[EE2]}{dt} = k_{EE2,{}^1O_2}[EE2][HO\cdot]_{SS} \qquad (8)$$

where [BZA], [EE2] and $[HO\cdot]_{SS}$ are the concentration of BZA, EE2 and HO·, respecvtively; $k_{BZA,HO\cdot}$ and $k_{EE2,HO\cdot}$ are the second-order rate constants between BZA, EE2 and HO·. After rearranging the Eqs. (7) and (8) gets:

$$\frac{1}{k_{BZA,{}^1O_2}} ln\frac{[BZA]_t}{[BZA]_0} =- \int [1O2]_{ss} \qquad (9)$$

$$\frac{1}{k_{EE2,{}^1O_2}} ln\frac{[EE2]_t}{[EE2]_0} =- \int [1O2]_{ss} \qquad (10)$$

Equating Eqs. (9) and (10) and rearranging leads to the competition kinetics relationship Eq. (11).

$$ln\frac{[EE2]_t}{[EE2]_0} = \frac{k_{EE2,HO\cdot}}{k_{BZA,HO\cdot}} \times ln\frac{[BZA]_t}{[BZA]_0} \qquad (11)$$

The liner regression of ln([EE2]/$[EE2]_0$) versus ln([BZA]/$[BZA]_0$) was shown in Figure S4. By employing the known second-order reaction rate constant between BZA and HO· (5.9 × 10^9 M^{-1} s^{-1}) [3], the second-order reaction rate constant between EE2 and HO· was calculated to be 1.09 × 10^{10} M^{-1} s^{-1}.

Detection of the reaction rate between EE2 and $^1O_2$

Second-order reaction rate between EE2 and $^1O_2$ was measured by using competition kinetics method. FFA, a commonly used competitor, was selected as the reference chemical competing with EE2 for $^1O_2$ in RB/air system (3.0 μM RB) at pH 8.0. The concentration of EE2 and FFA were controlled at 4.09 μM and 5.05 μM, reapectively. The result was listed in Table S2. According to the treatment for obtaining $[HO\cdot]_{SS}$, the competition kinetics relationship between EE2 and FFA could by depicted by Eq. (12).

$$ln\frac{[EE2]_t}{[EE2]_0} = \frac{k_{EE2,^1O_2}}{k_{FFA,^1O_2}} \times ln\frac{[FFA]_t}{[FFA]_0} \qquad (12)$$

The liner regression of $\ln([EE2]_t/[EE2]_0)$ versus $\ln([FFA]_t/[FFA]_0)$ was shown in Figure S5. By employing the known second-order reaction rate constant between $^1O_2$ and FFA (1.2×10^8 M^{-1} s^{-1}) [5], the second-order rate reaction constant between $^1O_2$ and EE2 was calculated to be 9.71×10^7 M^{-1} s^{-1}.

Table S1: The concentration variation of BZA and EE2 during the reaction period

Time (h)	BZA (μM)		EE2 (μM)	
	Experiment 1	Experiment 2	Experiment 1	Experiment 2
0.0	4.67	4.68	3.83	3.84
0.1	4.38	4.44	3.49	3.41
0.2	4.12	4.20	3.07	2.99
0.3	3.85	3.93	2.68	2.79
0.4	3.66	3.59	2.41	2.30
0.5	3.32	3.43	2.05	2.17

Table S2: The concentration variation of FFA and EE2 over the irradiation period

Time (h)	FFA (μM)		EE2 (μM)	
	Experiment 1	Experiment 2	Experiment 1	Experiment 2
0.0	5.07	5.03	4.09	4.08
0.1	4,20	4.27	3.49	3.56
0.2	3.89	3.75	3.31	3.15
0.3	3.57	3.49	3.07	3.02
0.4	3.25	3.41	3.88	2.96
0.5	3.19	3.30	2.89	2.78

Table S3: HPLC procedures* for EE2, BZA, FFA and 2-hTPA quantification

Chemicals	Mobile phase[a]		Flow Rate of Mobile Phase (mL/min)	Injection volume (µL)	Chromatographic Column	Wavelength of Detector (nm)		Retention Time (min)		LOQ (mg/L)	
	ACN#	Milli-Q				UV	FLR[b]	UV	FLR	UV	FLR
EE2#	60	40	1.0	50.0	★	-	236/310	-	2.25	-	0.02
BZA#	40	60	1.0	100.0	☆	224	-	1.71	-	0.04	-
FFA#	20	80	1.0	50.0	☆	218	-	1.62	-	0.03	-
2-hTPA#	33	67	0.8	100.0	☆	-	315/425	-	1.85	-	0.03

*all the detection methods were established by an Agilent 1260 series HPLC.

a pH of Mobile phase was adjusted to 8.0 ± 0.1 with H_2SO_4 and NaOH.

b detection wavelength (nm) of fluorescence detector: excitation/emission wavelength.

#: CAN, acetonitrile; EE2, 17α-ethinylestradiol; BZA, benzoic acid; FFA, furfuryl alcohol; 2-hTPA, 2-hydroxyl terephthalic acid.

★: ZORBAX SB-C18 reversed phase column (Agilent, 3.5 µm, 4.6 × 100 mm);

☆: CORTECS^{TM} C18 reversed phase column (Waters, 2.7 µm, 4.6 × 100 mm).

Table S4: Elemental composition, specific UV absorbance and ratio of specific absorption of HA

Index	Value
C	56.07%
O	33.75%
H	4.96%
N	3.28%
S	1.68%
Ash	0.26%
$SUVA_{254}$	5.06 L $(mg\ m)^{-1}$
E2/E3	2.63

Figure S1: (a) Photoreaction apparatus used in this study

(b) The relative intensity emitted by the source light

(c) The UV-vis absorption characteristics of HA, EE2, phenol

(d) The fluorescent property of HA

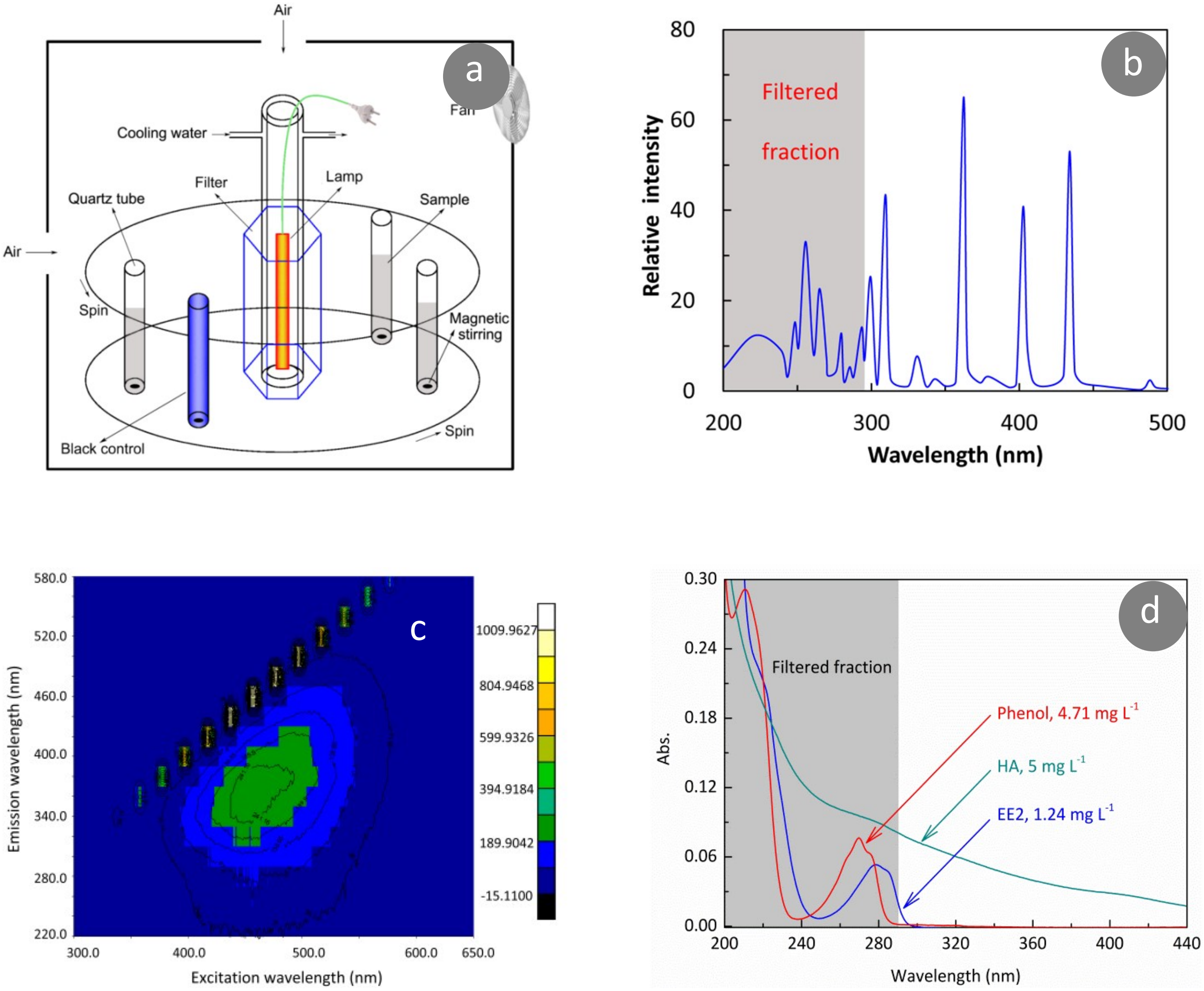

Figure S2: Formation rate of 2-hydroxyl terephthalic acid in HA/air solution at pH 8.0 ± 0.1

(The averaged data points and errors were based on duplicate experiments.)

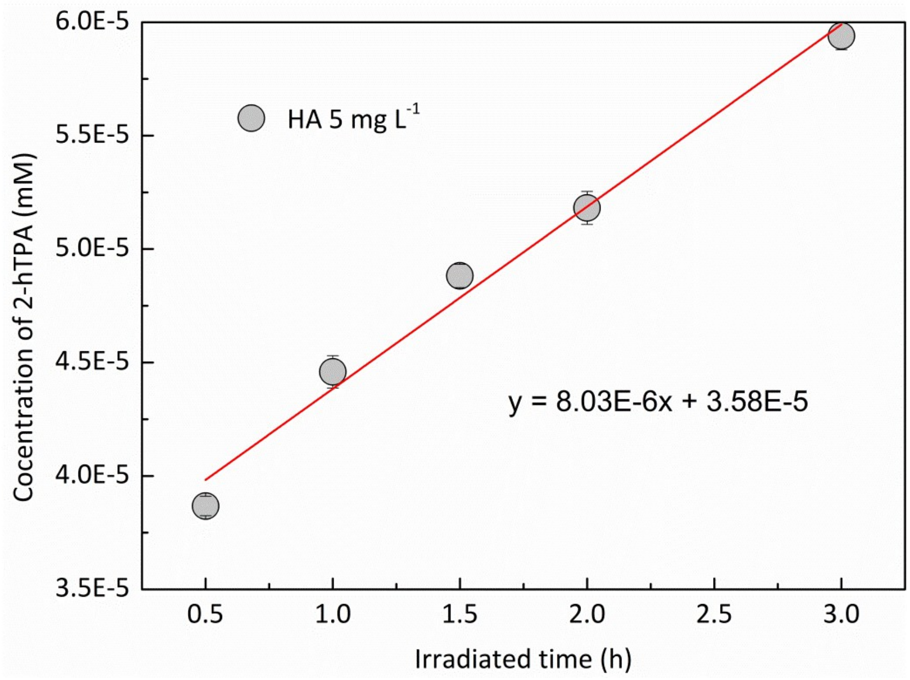

Figure S3: Photodegradation of FFA in Milli-Q water and HA system

(Both experiments were conducted at pH 8.0 ± 0.1 and under same air containing condition. The averaged data points and errors were based on duplicate experiments.)

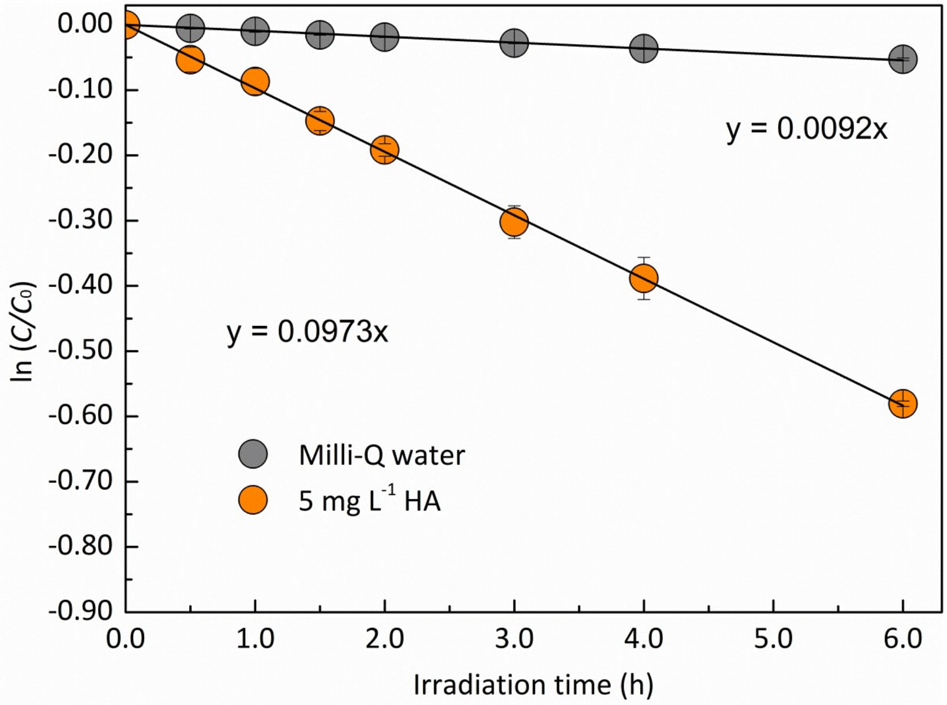

Figure S4: Correlation between ln([EE2]$_t$/[EE2]$_0$) and ln([BZA]$_t$/[BZA]$_0$) during competition reacting with HO· of EE2 and BZA in the Fe^{2+}/H$_2$O$_2$ system at pH 3.5 under black condition

(The slope of fitted liner represents the ratio of $k_{EE2,HO·}/k_{BZA,HO·}$. The averaged data points and errors were based on duplicate experiments.)

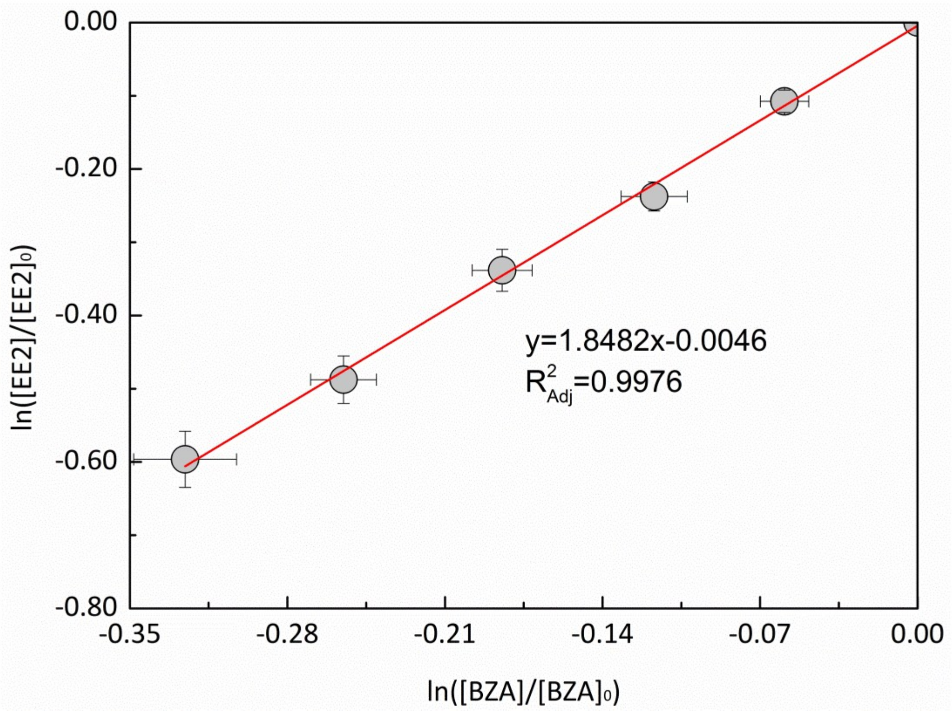

Figure S5: Correlation between ln([EE2]$_t$/[EE2]$_0$) and ln([FFA]$_t$/[FFA]$_0$) during competition reacting with $^1O_2$ of EE2 and FFA in the RB/air (2 Mm RB) system at pH 8.0 under irradiation

(The slope of fitted liner represents the ratio of $k_{EE2,1O2}/k_{FFA,1O2}$. The averaged data points and errors were based on duplicate experiments.)

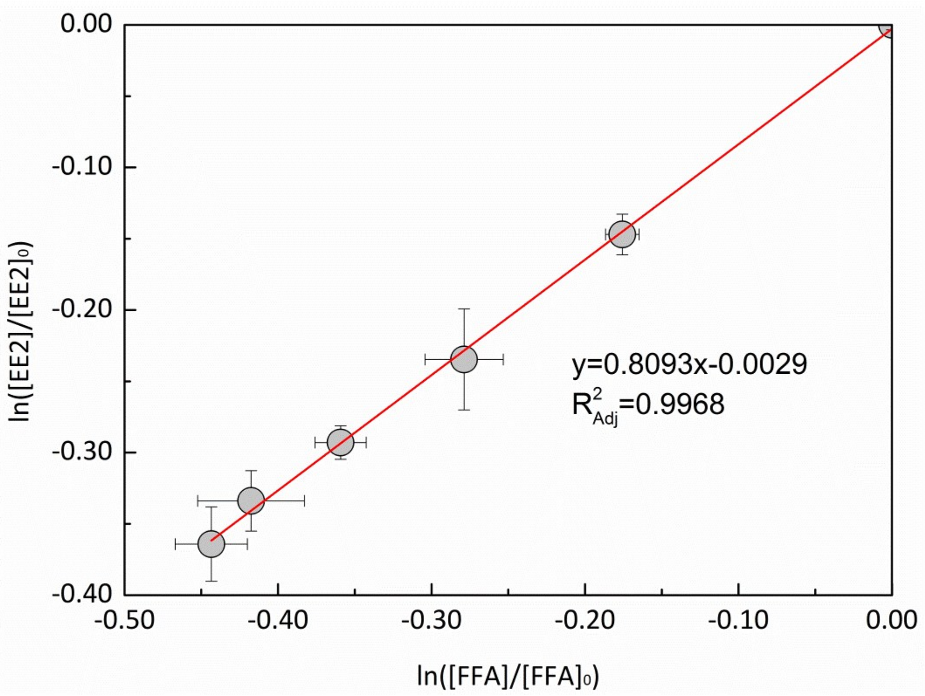

Figure S6: Light absorption characteristics of 5.0 mg L^{-1} HA in the range of 290-560 nm at different pH values

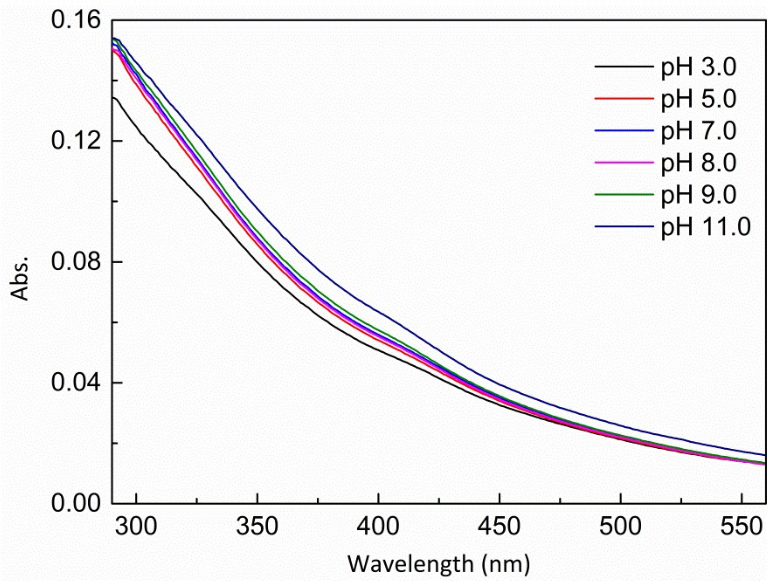

Figure S7: Detail information on EE2 photodegradation with different RS scavengers in 5.0 mg L^{-1} HA solutions

Degradation rate of EE2 in Milli-Q/Air system under pH 8.0

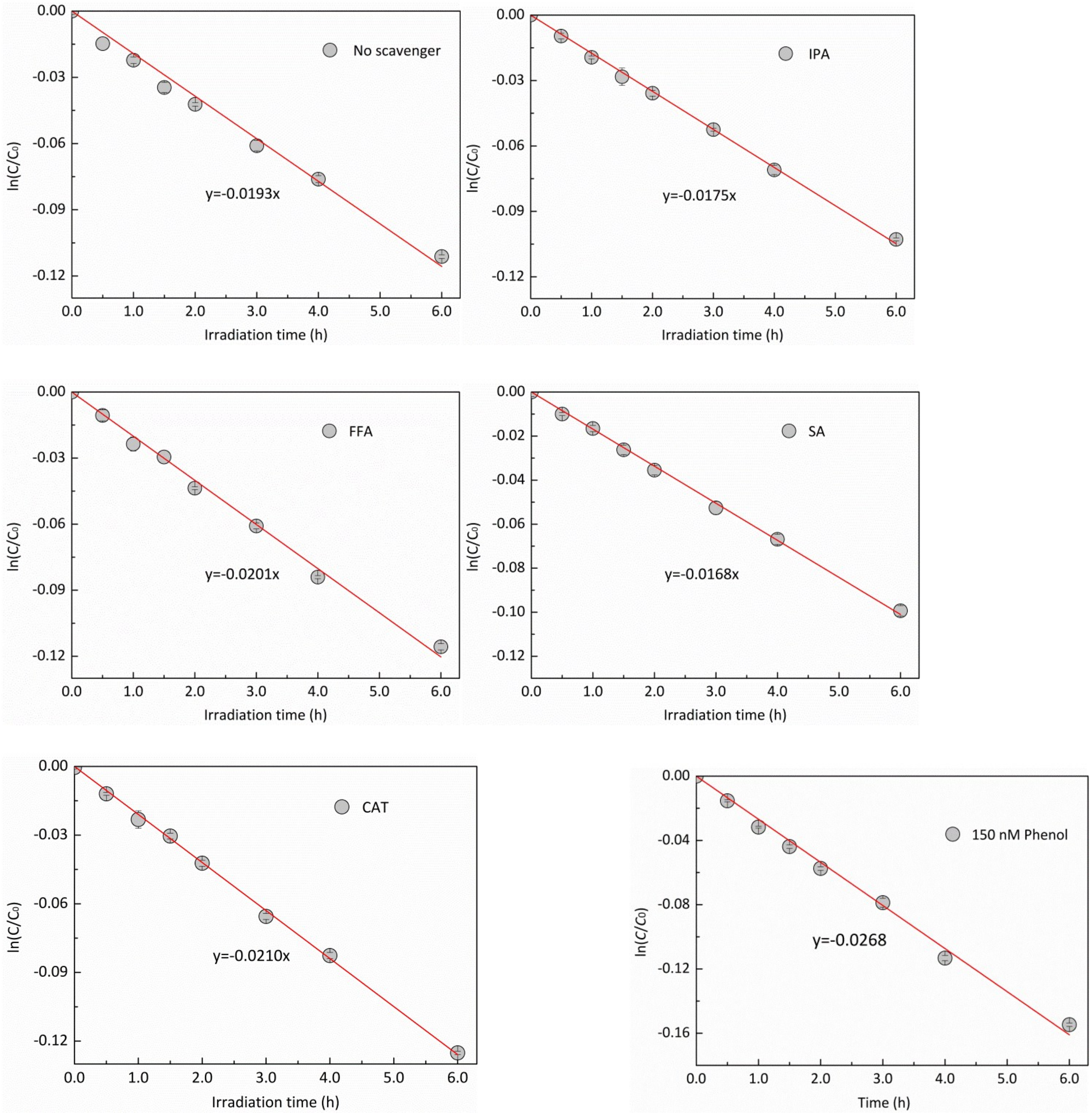

Degradation rate of EE2 in Milli-Q/Air system under pH 11.0

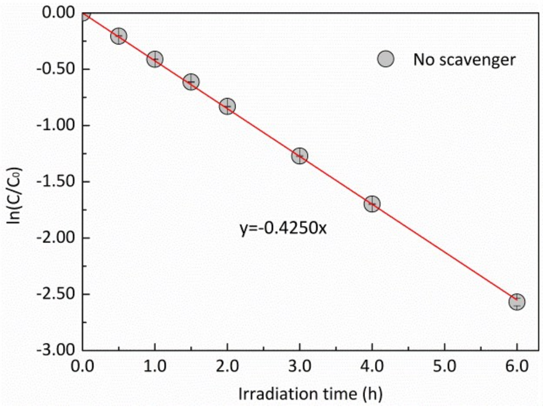

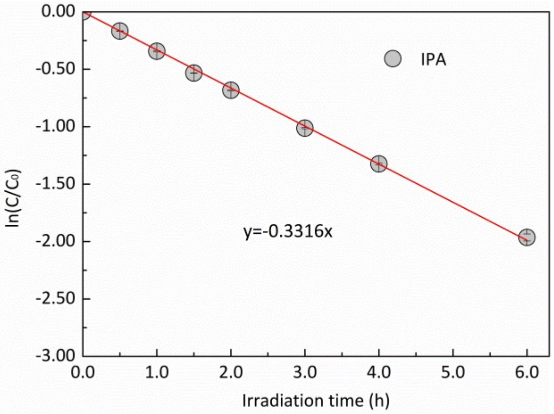

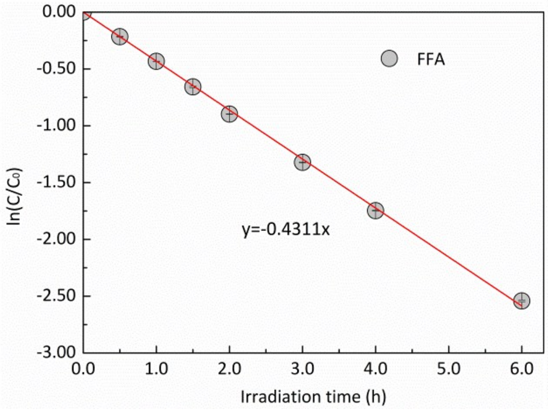

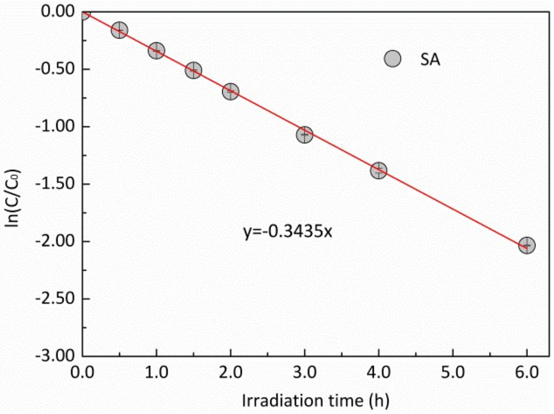

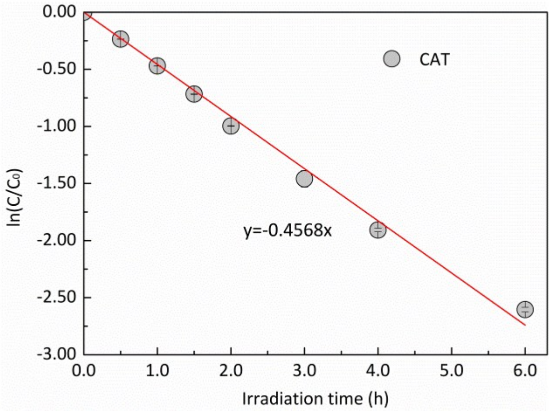

Degradation rate of EE2 in HA/Air system under pH 8.0

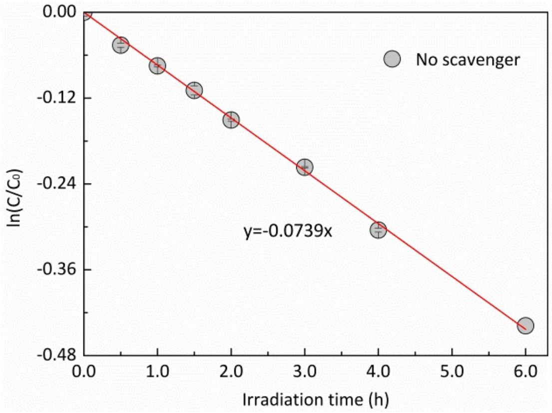

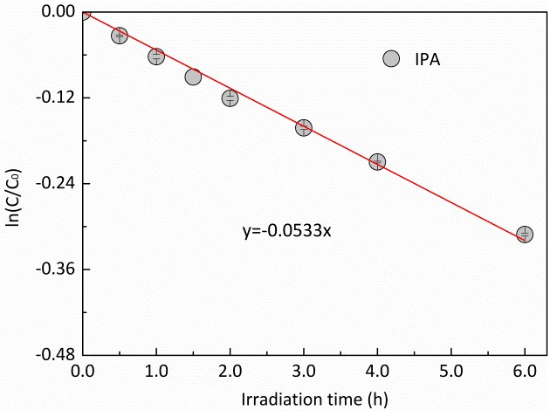

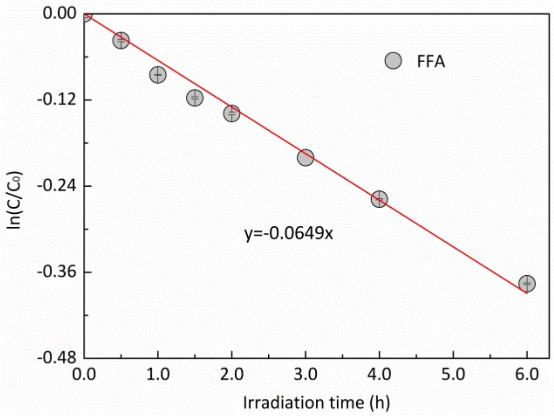

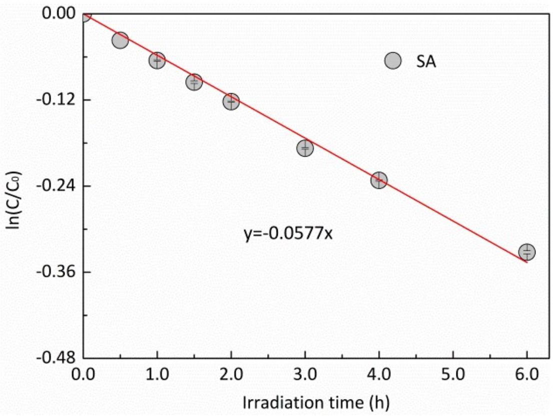

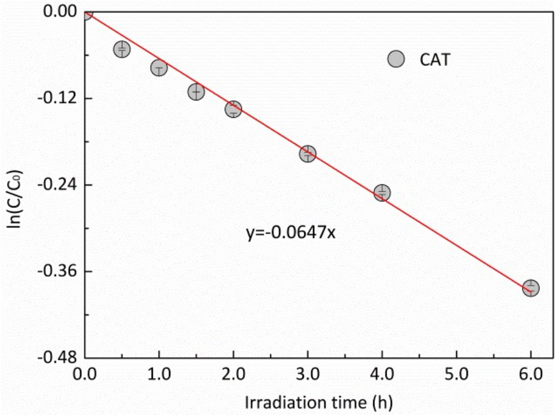

Degradation rate of EE2 in HA/Air system under pH 11.0

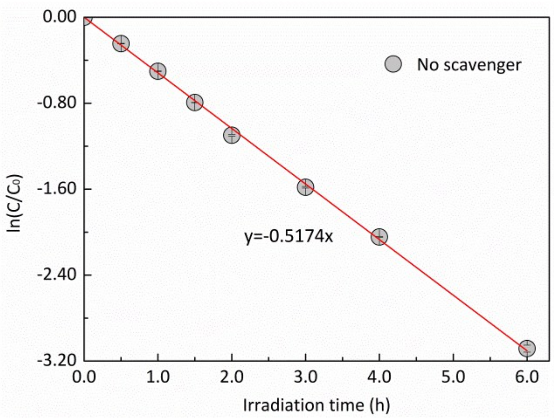

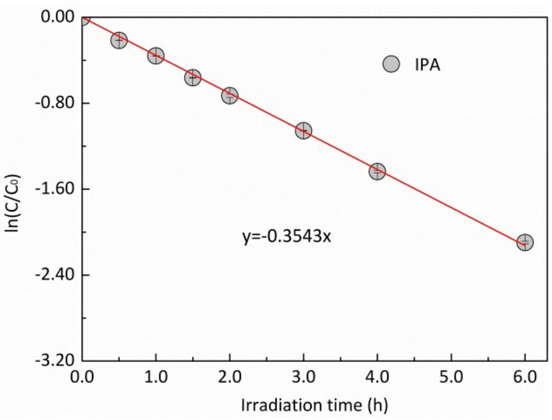

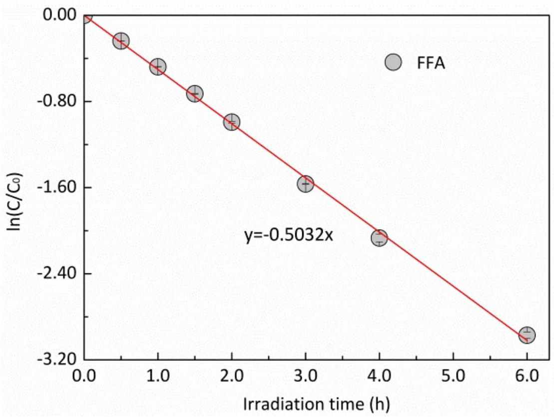

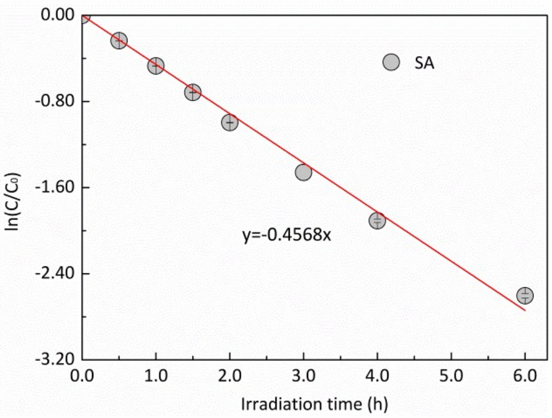

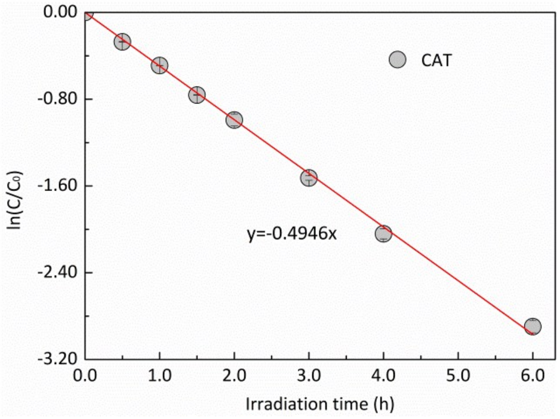

Degradation rate of EE2 in Milli-Q/N_2 system under pH 8.0

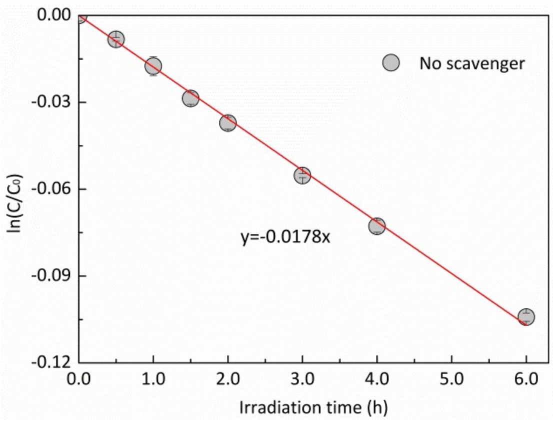

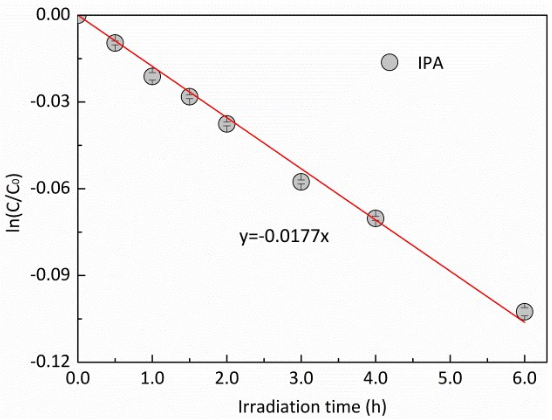

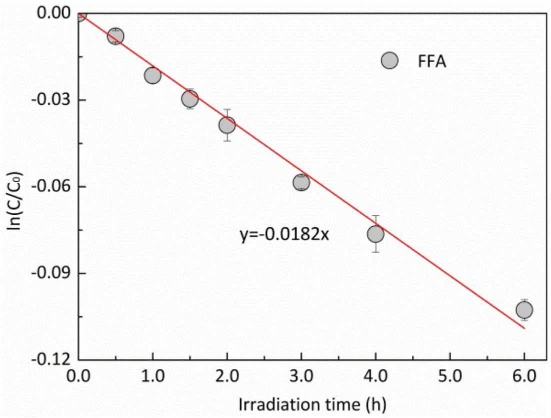

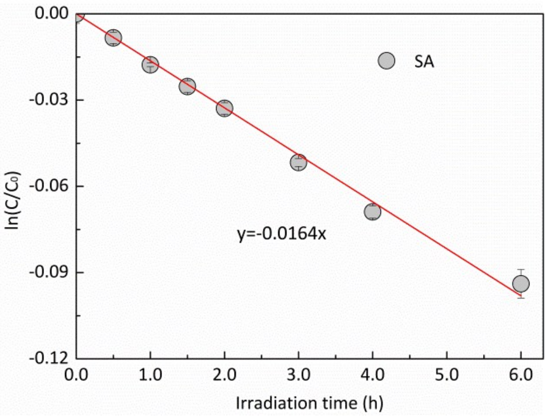

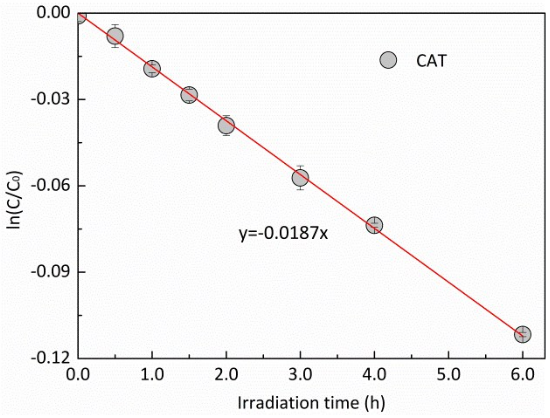

Degradation rate of EE2 in Milli-Q/O_2 system under pH 8.0

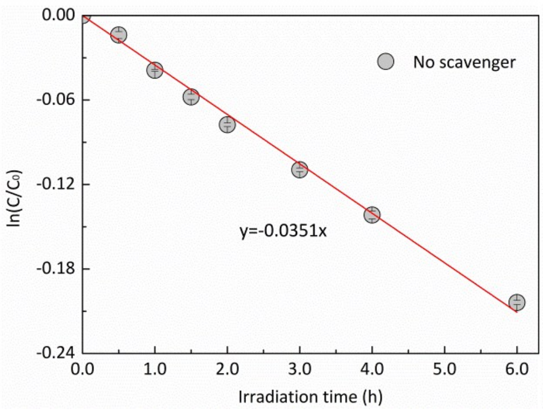

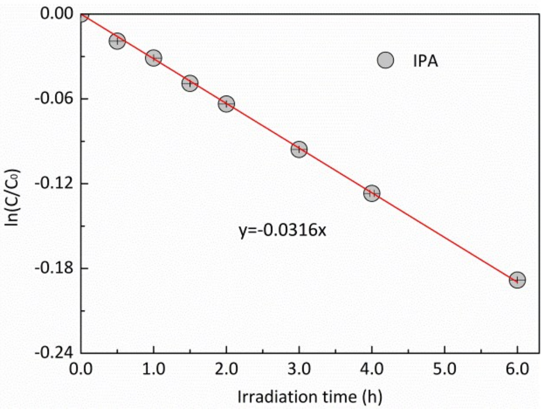

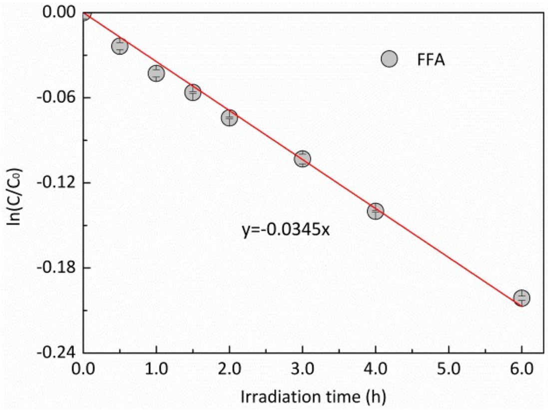

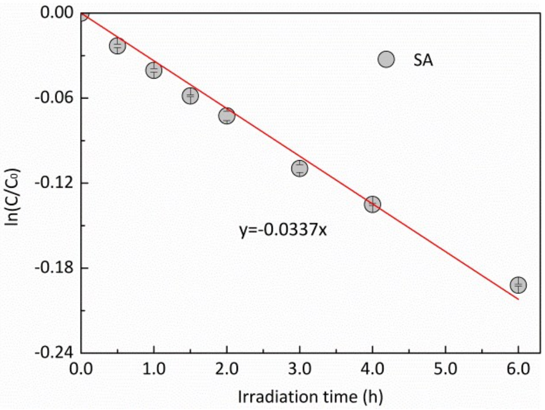

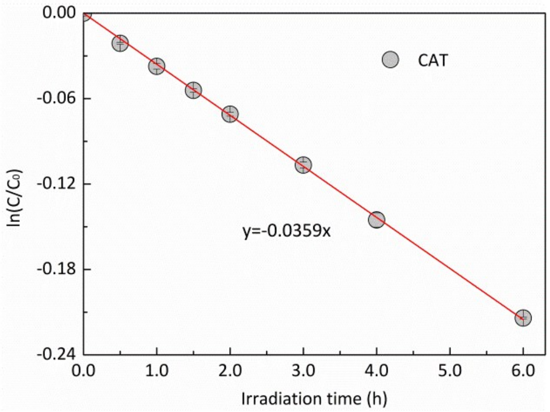

Degradation rate of EE2 in HA/N_2 system under pH 8.0

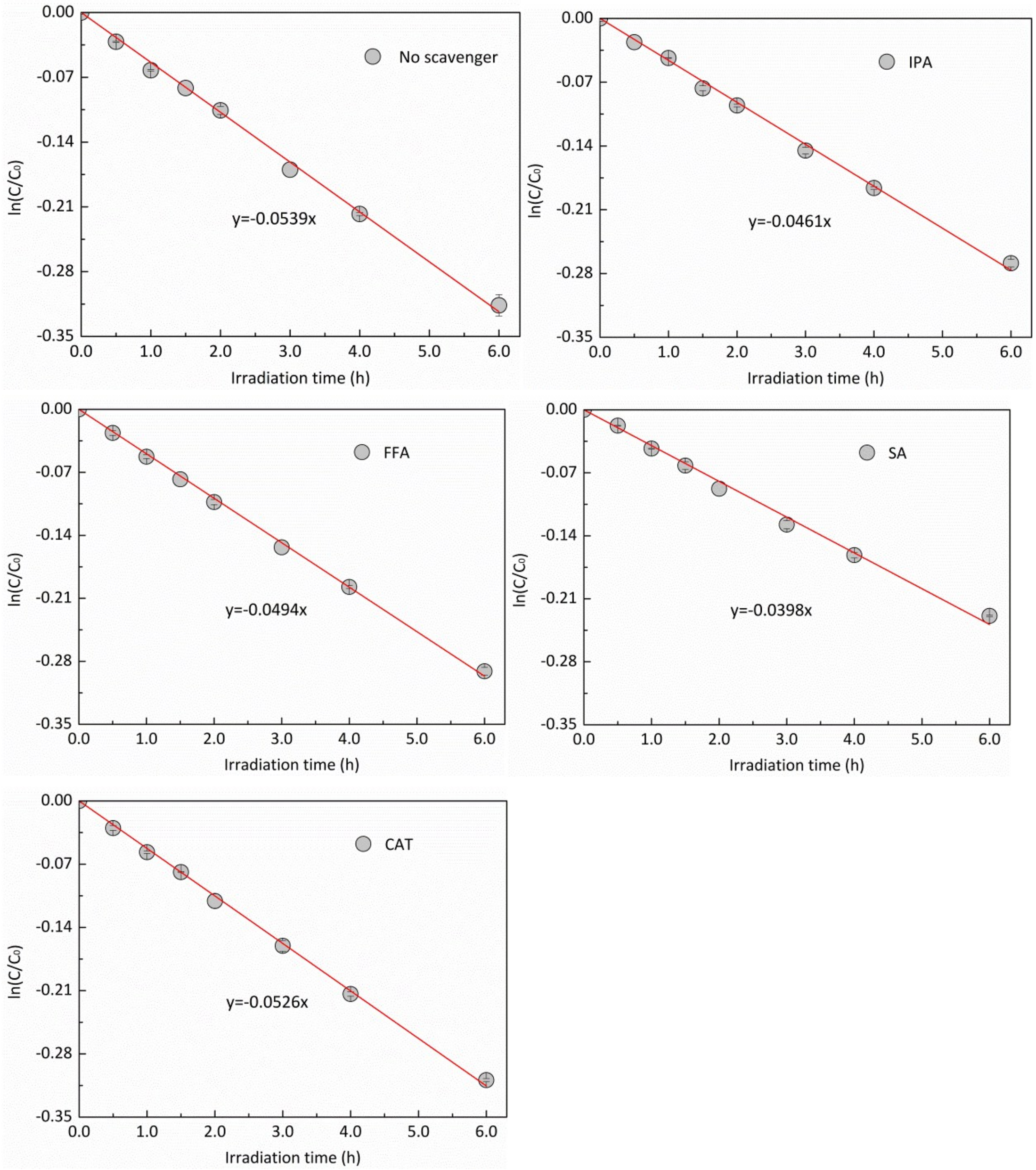

Degradation rate of EE2 in HA/O_2 system under pH 8.0

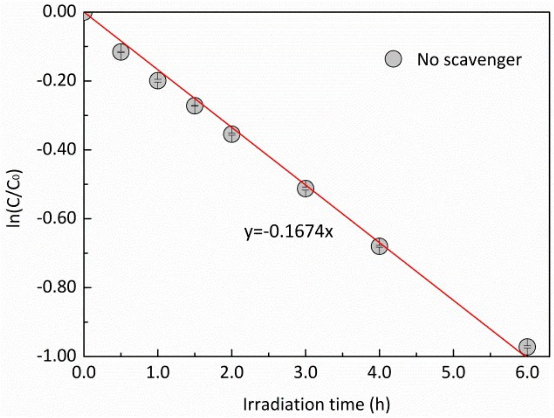

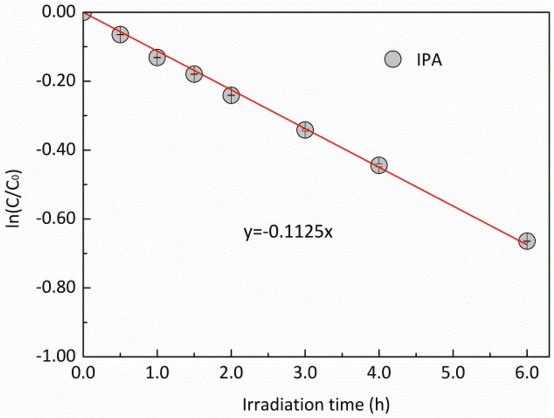

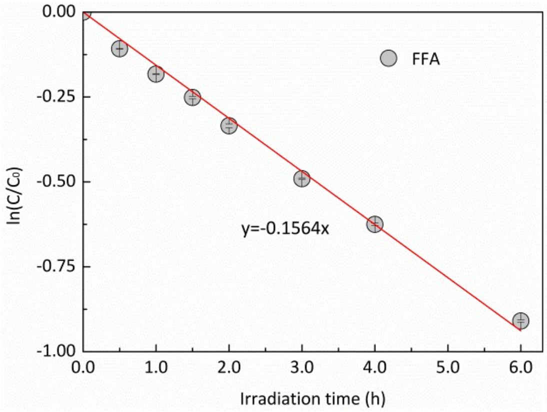

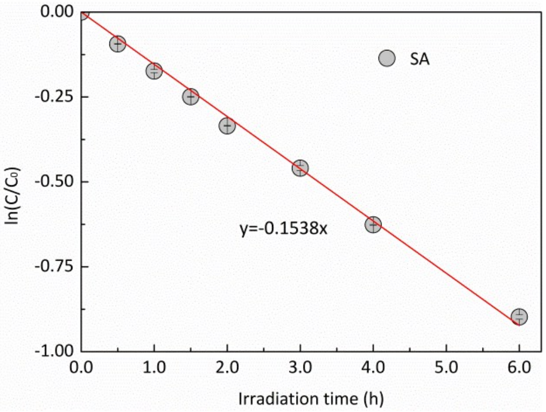

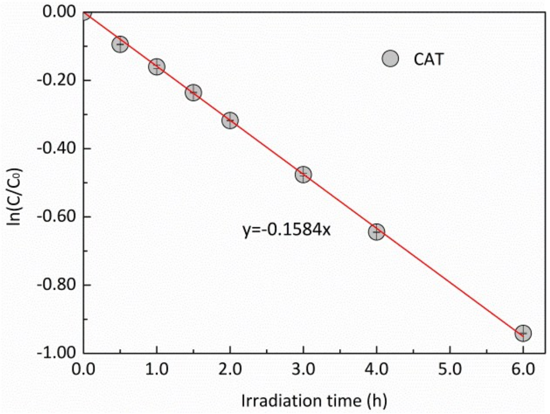

Literature cited

[1] G. Mark, A. Tauber, R. Laupert, H.-P. Schuchmann, D. Schulz, A. Mues, C. von Sonntag, OH-radical formation by ultrasound in aqueous solution–part II: terephthalate and Fricke dosimetry and the influence of various conditions on the sonolytic yield, *Ultrason. Sonochem.* 5 (1998) 41-52.

[2] S.E. Page, W.A. Arnold, K. McNeill, Terephthalate as a probe for photochemically generated hydroxyl radical, J. Environ. Monit. 12 (2010) 1658-1665.

[3] G.V. Buxton, C.L. Greenstock, W.P. Helman, A.B. Ross, Critical review of rate constants for reactions of hydrated electrons, hydrogen atoms and hydroxyl radicals ($\cdot OH/\cdot O^-$) in aqueous solution, J. Phys. Chem. Ref. Data 17 (1988) 513-886.

[4] J. Wenk, U. von Gunten, S. Canonica, Effect of dissolved organic matter on the transformation of contaminants induced by excited triplet states and the hydroxyl radical, Environ. Sci. Technol. 45 (2011) 1334-1340.

[5] W.R. Haag, E. Gassman, A. Braun, Singlet oxygen in surface waters—Part I: Furfuryl alcohol as a trapping agent, Chemosphere, 13 (1984) 631-640.